CHEMISTRY OF MATERIALS

Article

pubs.acs.org/cm

Activated CO_2 Sorption in Mesoporous Imidazolium-Type Poly(ionic liquid)-Based Polyampholytes

Sebastian Soll, Qiang Zhao, Jens Weber,* and Jiayin Yuan*

Department of Colloid Chemistry, Max Planck Institute of Colloids and Interfaces, Research Campus Golm, D-14476 Potsdam, Germany

Supporting Information

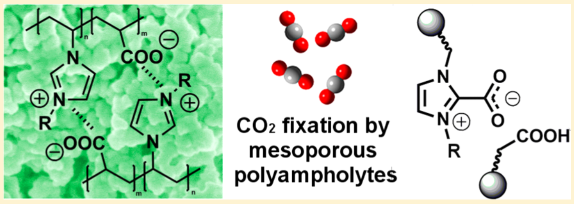

ABSTRACT: In this contribution, we present the formation of mesoporous polyampholyte networks via self-complexation (inter- and intrapolyelectrolyte complexation) of copolymers bearing both the imidazolium cations and the carboxylic acid units. The copolymers were prepared via straightforward free radical copolymerization of acrylic acid and vinylimidazolium-based ionic liquid monomers possessing different alkyl substituents in DMSO at 80 °C. Nitrogen adsorption measurements and electron microscopy were used to examine the porous structures. The Brunauer−Emmett−Teller (BET) specific surface areas of the resulting mesoporous complexes were measured to be up to 260 m^2/g and varied in terms of the complexation solvent quality, the copolymer composition, and the precipitation concentration of copolymers as well as the chemical structure of the employed ionic liquid monomers. The CO_2 sorption behavior of a selected mesoporous polyampholyte was studied in detail. It could be shown that two processes are effective: adsorption at the external surface and absorption into the polymer matrix. Fourier transform infrared (FTIR) spectroscopy gave hints that the absorption process comes along with the formation of imidazolium-carboxylates, presumably via a transient N-heterocyclic carbene intermediate.

KEYWORDS: *polyampholyte, poly(ionic liquid), polyelectrolyte complex, CO_2 sorption, mesoporous materials, N-heterocyclic carbenes*

1. INTRODUCTION

Recently poly(ionic liquid)s or polymerized ionic liquids (PILs) as a subclass of polyelectrolytes have attracted rapidly increasing attention in the field of polymer and materials science.[1−5] They are commonly prepared by straightforward polymerization of monomeric ionic liquids (ILs). The presence of an IL moiety in the polymer repeating unit integrates some IL properties with the polymeric architecture, therefore expanding the traditional application spectrum of conventional polyelectrolytes studied so far. Some application examples of PILs have already been demonstrated very recently, such as solid polymeric electrolytes, stationary phases in chromatography, carbon precursors, catalysis, etc.[6−13]

Polyampholytes are charged macromolecules containing both positive and negative charges along their polymeric chains.[14−17] Three different categories can be distinguished in polyampholytes generally: quenched, annealed, and zwitterionic ones. The first are permanently charged regardless of the solution pH, while in the second class the net charge and the charge distribution depend on the pH value of the solution. Zwitterionic polyampholytes have oppositely charged ion pairs localized on one pendant substituent. Typical polyampholytes were prepared from charged anionic or cationic monomers, acidic and basic vinyl monomers, zwitterionic monomers, or ion-pair comonomers. Since the first study of synthetic polyampholytes in 1950, they have drawn widespread attention and interest in the fields of polymer chemistry and physics, molecular biology, colloid chemistry, coordination chemistry, and catalysis. Their application spectrum covers model systems for electrostatic interactions and structural organization in proteins, secondary oil recovery, water desalination, recovery of metal ions, and drag reduction. So far, the research scope on polyampholytes focuses majorly on their particular physics in aqueous solutions and the corresponding theory and simulation.[18−20] In comparison, the solid state properties and function of polyampholytes attract somehow rare attention, not to mention mesoporous solid polyampholytes. Introducing mesopores (pore sizes between 2 and 50 nm) would provide sufficiently high surface area and satisfactory mass/energy transfer at the same time.[21,22] So far, mesoporous poly(ionic-liquid) copolymers, containing alternate charges along their single polymeric chains, i.e. mesoporous polyampholytes, have not been reported to the best of our knowledge. From a practical application point of view, mesoporous polyampholytes represent a logic pathway to improve and amplify their material functions.

Herein, we describe a facile template-free synthetic route to mesoporous polyampholytes from PIL-based copolymers as a single structural building component via self-complexation in organic solvents, in contrast to common polycation-polyanion binary systems in aqueous solutions. The polyampholyte copolymers were prepared via conventional free radical

Received: March 20, 2013
Revised: July 1, 2013

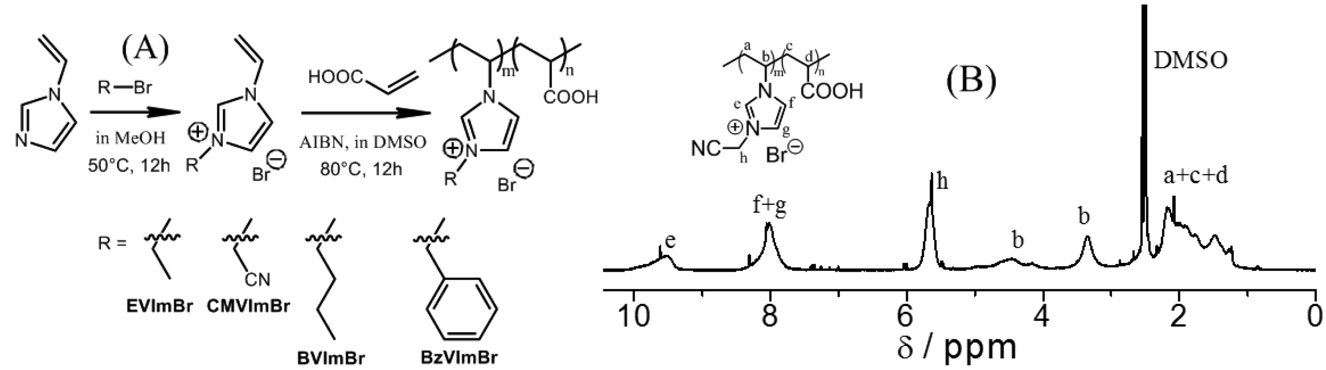

Figure 1. (A) The synthetic scheme of polyampholytes P(XVImBr$_y$-co-AA) from copolymerization of acrylic acid and four vinylimidazolium-based ionic liquid monomers in DMSO; (B) ^{1}H NMR of P(CMVImBr$_{1.03}$-*co*-AA) in DMSO-d_6. The peak at 2.5 ppm is the residue DMSO peak.

polymerization of acrylic acid with IL monomers of different structure types in DMSO at 80 °C. The as-synthesized polyampholytes formed a solid mesoporous matrix via inter/intrapolyelectrolyte complexation when precipitated in ammonia-containing organic solvents. The process is triggered by in situ deprotonation of the carboxylic acid groups in the same copolymer chain. The copolymer composition, the concentration of polymer solutions, and the quality of the complexation solvents (defined as different organic solvents in which complexation took place) were systematically varied to reveal the influence of the experimental parameters on the pore structures. It should be mentioned that many porous PIL-based materials reported to date are macroporous (pore size >50 nm) with specific surface area up to 37 m^2 g^{-1}.[23−25] Mesoporous PIL-based systems with specific surface area up to 310 m^2 g^{-1} were reported only recently via a hard-templating synthetic approach or via an interpolyelectrolyte complex mechanism.[26−28] Mesoporous materials based on layer-by-layer assembly of polyelectrolytes have been reported before as well, but templates were necessarily required in order to imprint substantial mesoporosity in most cases.[29,30]

Additionally and also within the focus of the present paper, there has been a large interest in the CO$_2$ adsorption properties of (polymerized) ionic liquids, mostly in the bulk.[9] The present system combines a straightforward synthesis with high surface areas in the final product, which makes it indeed a suitable candidate for CO$_2$ utilization. Previous reports have shown that, although not competitive in terms of capacity, PILs seem to have some kind of intrinsic CO$_2$-philicity. This feature makes them interesting as it provides some added benefit over purely adsorptive systems such as activated carbons. Yet, the adsorption properties are not fully understood, and it is hence the aim of the present paper to provide insight into the finer details of CO$_2$ sorption in PIL-based porous materials.

2. EXPERIMENTAL SECTION

Materials. Lithium bis(trifluoromethanesulfonyl)imide (LiTf$_2$N, 99.95%), potassium hexafluorophosphate (KPF$_6$, 97%), 1-vinylimidazole (99%), bromoethane (98%), bromoacetonitrile (97%), 1-bromobutane (99%), benzyl bromide (98%) and acrylic acid (AA, 99%) were purchased from Sigma-Aldrich and used without further purification. 2,2′-Azobis(2-methylpropionitrile) (AIBN, 98%) was recrystallized from methanol. 1-Ethyl-3-vinylimidazolium bromide (EVImBr), 1-butyl-3-vinylimidazolium bromide (BMVImBr), 1-cyanomethy-3-vinylimidazolium bromide (CMVImBr), and 1-benzyl-3-vinylimidazolium bromide (BzVImBr) were synthesized according to the previous literature.[31−33] All the solvents used in this study were of analytic grade.

Synthesis of Copolymers of Acrylic Acid and Ionic Liquid Monomers. The copolymers were prepared via conventional free radical copolymerization of the corresponding ionic liquid monomer and acrylic acid (AA) in a feeding ratio close to 1.5:1. For the copolymerization made up of CMVImBr (see Figure 1 for chemical structure) and AA, several additional feeding molar ratios (5:1, 3.5:1, 2:1, 1:1.5, 1:2, and 1:3) were tested to create a copolymer toolbox with the same building units yet a series of compositions. Here, the procedure to prepare the copolymer P(CMVImBr-*co*-AA) from CMVImBr and AA at a feeding molar ratio of 1.5:1 is introduced as an example. 4.05 g (0.019 mol) of CMVImBr, 0.87 mL (0.0127 mol) of acrylic acid, 100 mg (0.6 mmol) of AIBN, and 50 mL of DMSO were added in a 100 mL flask. After complete dissolution of the solid, the mixture was deoxygenated by four cycles of freeze−pump−thaw process. After being backfilled with argon, the flask was stirred in an oil bath thermostatted at 80 °C for 15 h. After cooling down, the reaction mixture was added dropwise into an excess of diethyl ether. The precipitate was redissolved in DMSO and precipitated again in acetone. After filtering off, the product was dried under vacuum at 60 °C till constant weight. The chemical structures were confirmed by ^{1}H NMR spectra in Figure 1. The composition was determined by elemental analysis.

Anion Exchange of the Synthesized Copolymer. In a typical anion exchange process (taking Tf$_2$N$^-$ as an example), copolymers with Br$^-$ anion (10 g/L) were dissolved in deionized water. An aqueous solution of LiTf$_2$N (50 g/L) was added dropwise into the copolymer solution to reach a molar ratio of [Tf$_2$N]/[Br] = 1.15. After addition, the stirring continued for 3 h. The solid precipitate was separated by filtration and washed several times with deionized water and dried at 90 °C by high vacuum overnight.

Preparation of Mesoporous Polyampholytes. In a typical run, P(CMVImBr-*co*-AA) was dissolved in DMSO solvent at a designed concentration at room temperature to form a transparent solution. Thirty mL of diethyl ether (complexing solvent) containing 0.5 wt % of NH$_3$ (prepared by using 3.5 g of 2 M NH$_3$ in isopropanol) was placed in a glass beaker, into which 2 mL of the copolymer solution was dropped (speed: 3 mL/min) under a stirring rate of 900 rpm and sonication (40% sonication amplitude of a Bandelin Electronics Sonorex RK 100 ultrasonic bath). The sonication was kept for 1 min after the addition was finished. The upper liquid phase was discarded, and the solid content was collected, washed by diethyl ether four times, and dried under vacuum at 50 °C for 12 h.

Characterization Methods. ^{1}H nuclear magnetic resonance (^{1}H NMR) measurements were carried out at room temperature using a Bruker DPX-400 spectrometer operating at 400.1 MHz. DMSO-d_6 and D$_2$O were used as solvents. Elemental analysis was performed for carbon, hydrogen, and nitrogen using a Vario EL Elementar. Field emission scanning electron microscopy (FESEM) observations were performed on a LEO 1550-Gemini instrument. The samples were loaded on carbon coated stubs and coated by sputtering a Au/Pd alloy prior to imaging. X-ray diffraction experiments were done with a Bruker D8 diffractometer using Cu K$_\alpha$ radiation (λ = 0.154 nm) and a

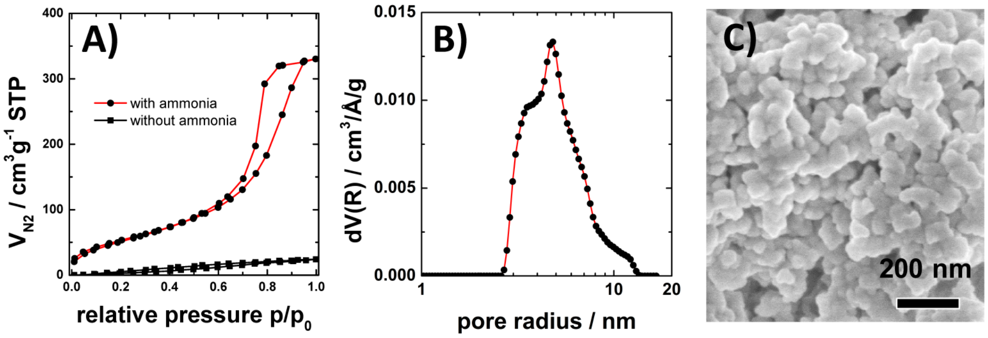

Figure 2. Nitrogen adsorption/desorption isotherm (A), pore size distribution curve obtained by QSDFT analysis of the adsorption branch (B), and SEM image (C) of a mesoporous polyampholyte product prepared from P(CMVImBr$_{1.03}$-*co*-AA).

scintillation counter. FT-IR spectra were performed on a BioRad 6000 FT-IR spectrometer; samples were measured in solid state using a Single Reflection Diamond ATR.

Nitrogen (N_2) sorption experiments were performed with a Quantachrome Quadrasorb machine at liquid nitrogen temperature (77.4 K), and initial data analysis was performed using the Quadrasorb 5.05 software package (Quantachrome Instruments). The surface area and pore volume were calculated using the Brunauer–Emmett–Teller (BET) equation and the Barrett–Joyner–Halenda (BJH) method, respectively. CO_2 adsorption was measured at 273 or 283 K using a Quantachrome Autosorb-MP1 machine. Different measurement modes were used with respect to the allowed equilibration times. Measurements using an equilibration time of 3 min (the time interval, in which the pressure change must be below the allowed difference, typically $\Delta p < 0.0008$ atm) are designated as "fast" CO_2 adsorption. An equilibration time of 3 min is a commonly used "default" value of Quantachrome Instruments. We also used the maximum setting of the equilibration time (99 min). Those measurements are designated as "slow" measurements. A detailed explanation can be found in the Supporting Information. High-purity gases were used in all cases. All samples were degassed at 80 °C for 20 h before gas adsorption measurements.

3. RESULTS AND DISCUSSION

Figure 1A shows the chemical structures and the general synthetic route to several polyampholyte copolymers, which contain both cationic vinylimidazolium units and carboxylic acid groups along each polymer chain. Four ionic liquid (IL) monomers were chosen in this study to prove the general concept of mesoporous polyampholytes. They were synthesized via quaternization of 1-vinylimidazole with corresponding alkyl bromides. Here, the R group on the vinylimidazolium cation varies from short cyanomethyl and ethyl chains to long and large *n*-butyl and benzyl species.

The copolymers were readily prepared in one step via free radical copolymerization of acrylic acid and aforementioned IL monomers in DMSO at 80 °C. For reasons of simplicity, the IL monomers were denoted as *X*VImBr, and their copolymers as P(*X*VImBr$_y$-co-AA), where X = E, CM, B, and Bz refer to the ethyl, cyanomethyl, *n*-butyl, and benzyl substituents, while y is the molar ratio of [imidazolium]/[COOH] in the copolymer chains.

The use of DMSO as reaction medium is very crucial as it provides good solubility to the formed copolymers and at the same time keeps the carboxylic acid groups in an associated state. In dependence of the solvent quality and the [imidazolium]/[COOH] ratio, these copolymers could be either positively or negatively charged, i.e. they are annealed polyampholytes. For example, in organic solvents or in neutral or acidic aqueous solutions the acrylic acid units are dominantly in a protonated form, thus the overall net charge is positive and governed only by the imidazolium fraction. In contrast in basic organic media deprotonation of the COOH groups takes place and the [imidazolium]/[COOH] ratio determines the final charge of the polyampholytes. In this study we made use of the unique combination of the strong imidazolium cation and the pH dependent carboxylate electrolyte in exactly the same copolymer chain for the preparation of porous polyampholytes. While the following part will present the synthesis of the various polymers, only the cyanomethyl system will be discussed and analyzed in detail within the second part of the manuscript.

The success in the synthesis of each copolymer was confirmed by elemental analysis and proton nuclear magnetic resonance spectra (^{1}H NMR, see the SI for full characterization details). Elemental analysis was conducted here to each copolymer to access the realistic composition, because the severe overlapping of the copolymer backbone protons in poly(acrylic acid) (PAA) and PIL components makes NMR characterization alone inaccurate to estimate the exact ratio. After some fine-tuning in the experiment parameters, a close-to 1:1 molar ratio of [imidazolium]/[COOH] was reached in all four types (Tables S1 and S2). Figure 1B shows the characteristic ^{1}H NMR spectrum of P(CMVImBr$_{1.03}$-*co*-AA). The broad multisignals in the range of 1.0 to 2.7 ppm are assigned to the backbone protons of both PAA and PIL components except the methine [$-CH_2$-***CH***(N)-CH_2-] one close to the nitrogen atom. This proton signal shifts to the low field as two splitted sets at 3.3 and 4.4 ppm. The [-***CH***$_2$CN] methylene protons appear at 5.6 ppm. Signals at 9.0 and 8.5 ppm correspond to the imidazolium ring protons of [>N***C******H***N<] and [>N***CH******C******H***N<], respectively. All in all, the ^{1}H NMR spectra and EA results verify the chemical structure and composition of the copolymers.

In our attempt to construct the porous polyampholyte networks, we first tested P(CMVImBr$_{1.03}$-*co*-AA) in various experimental conditions. The copolymer was initially dissolved at a concentration of 0.9 wt % in DMSO, where the COOH units are existent in an associated status. At this stage, no or only weak complexation occurred, and the solution appeared transparent and homogeneous. This solution was dropwise added into an excess of diethyl ether containing 0.5 wt % of ammonia under ultrasound treatment. Under this basic condition the COOH groups in the copolymer chains were deprotonated into COO^-, which in turn brings to an in situ ionic complexation between the cationic imidazolium units and the COO^- anions. Note that both the cation and the anion precursor (the acid form of COOH) are present in the same

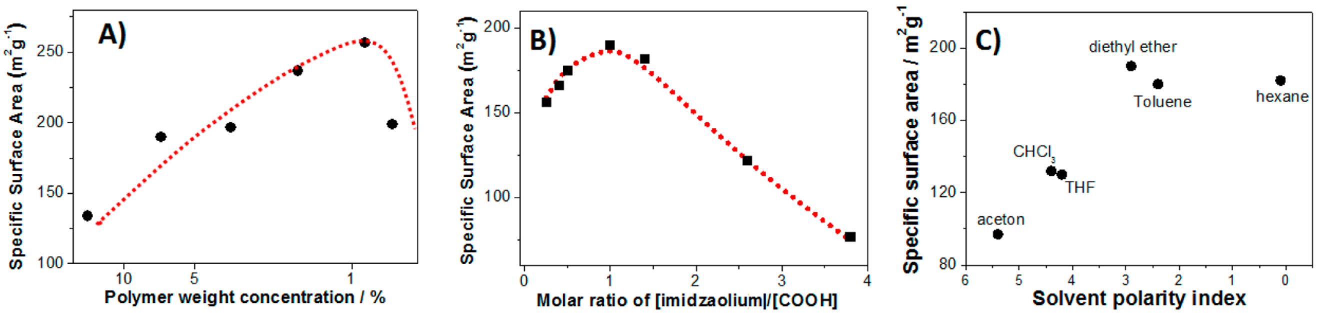

Figure 3. (A) Plot of S_{BET} of mesoporous polyampholytes from P(CMVImBr$_{1.03}$-*co*-AA) vs the copolymer concentration in DMSO used for sample preparation. The dotted red lines are a guide to the eye. (B) Plot of S_{BET} vs the copolymer composition. (C) Plot of S_{BET} of mesoporous polyampholytes from P(CMVImBr$_{1.03}$-*co*-AA) vs solvent polarity index.

copolymer in a quasi-equivalent molar ratio, so a homogeneous mixing of these two species has been reached at a molecular level already before the complexation took place. A diffusion process, which is usually quite important in a common polycation-polyanion binary interpolyelectrolyte complex system, is thus minimized in the current system. The driving force for the ionic complexation is the entropy gain resulting from the release of the low molecular ammonium bromide salt, in which the bromine anion and ammonium cation were previously associated with the imidazolium cation and the carboxylate anion in the copolymer chains. The ammonium bromide salt was however not detected in the product, as the X-ray diffraction analysis excludes its existence. In our experiment, the diethyl ether was mixed with 10% of isopropyl alcohol (from the ammonia solution) and 7% of DMSO (from the copolymer solution), which seems to dissolve the in situ formed salt. The complex precipitated still in this solvent mixture, which was separated and washed 5 times with diethyl ether before drying in a vacuum oven at 50 °C for 12 h.

Figure 2A shows the nitrogen adsorption/desorption isotherm of the as-synthesized porous polyampholytes based on P(CMVImBr$_{1.03}$-*co*-AA). It exhibits ambiguously a type-IV isotherm with a hysteresis loop in the P/P_0 range from 0.6 to 0.9. The pore size distribution curve (determined by quenched solid density functional theory, QSDFT, adsorption branch, cylindrical pores, Figure 2B) indicates that the porosity of the material is essentially made up of mesopores having radii from 6 to 12 nm. The specific surface area calculated from Brunauer−Emmett−Teller equation (S_{BET}) is 260 m^2 g^{-1} and the pore volume of this material is 0.49 cm^3 g^{-1}. It must be stated that ammonia controlled strictly the complexation process. Without ammonia activation, the ion pairing of the imidazolium and carboxylate did not occur, and the product was essentially nonporous (Figure 2A) and remained soluble in DMSO.

Finally, it should be noted that the preparation of the mesoporous polyampholytes is also possible in the absence of ultrasonic irradiation. The porosity is however reduced by ∼15% (see Figure S7 for exemplary results).

An image recorded from the scanning electron microscopy (SEM) of the porous complex is shown in Figure 2C. Primary particles of sizes around 50 nm are observed, which seem to be agglomerated into large species. The observed porosity can consequently be attributed to the void spaces in-between the formed nanoparticles. These particles are physically cross-linked and stabilized by strong electrostatic interaction between the cationic imidazolium units and the anionic COO^- groups in the copolymer.

The pore generation in this approach coincides with a series of events, i.e. the deprotonation of the COOH groups, followed by complexation and precipitation. It is not surprising that the porous structure and the S_{BET} values of the complex are dependent on the exact preparation conditions, for example, the copolymer concentration, the copolymer composition, the complexation solvent, etc. By variation of the P(CMVImBr$_{1.03}$-*co*-AA) copolymer concentration in DMSO, the S_{BET} of the resulting material could be tuned with a maximal value of 260 m^2 g^{-1} at a concentration of 0.9 wt % (Figure 3A). The S_{BET} value is comparable with the previously reported ones for porous complexes formed between a PIL and PAA.[26] Above this concentration, the S_{BET} value drops smoothly. Nevertheless, the volumetric yield increases, as a concentrated solution holds more polymers. To study the composition effect, seven P(CMVImBr-*co*-AA) copolymers of the [imidazolium]/[COOH] molar ratios in the range of 3.80 to 0.26 were tested at a fixed copolymer concentration of 7 wt % in the same procedure. The S_{BET} values of the porous products were plotted against the [imidazolium]/[COOH] ratio. As shown in Figure 3B, the highest S_{BET} value peaks at a composition of [imidazolium]/[COOH] = 1. This is understandable, because at this optimal condition the population of the cations and anions is in fact identical, facilitating a maximum ion complexation. The effect of different complexation solvents is shown in Figure 3C. Hereby the solvent polarity index could be considered as an important parameter for the formation of the mesoporous structure. Though the complex products are nonporous in polar solvents, like methanol or ethanol, the S_{BET} value increases in less polar or nonpolar solvents with decreasing polarity index from acetone (95 m^2/g) to chloroform (135 m^2/g) and THF (130 m^2/g) and further to diethyl ether (230 m^2/g). A plateau is reached below a polarity index of 3, a typical value for nonpolar solvents like toluene and hexane. These are poor solvents for the copolymer, which are beneficial to develop the mesoporous network and minimize the chain motion. The chemical structure is another important factor that affects the pore characteristics. Table 1 summarizes the influence of the alkyl substituent on the imidazolium ring and various anions on the S_{BET} values of the formed products. S_{BET} decreases with increasing steric hindrance of group R (Entries 1−4), when keeping the same anion (Br^-). It seems that the ionic complexation is partially screened when bulky groups are attached to the imidazolium ring. The highest values are obtained in the case of the ethyl group, while a longer aliphatic butyl chain or an aromatic benzyl group leads to a reduced specific surface area. On the contrary exchange of the counteranion has little to no effect.

Table 1. Specific Surface Area in Dependence of Counter Anions and Alkyl Substituents in the Polyampholyte (Prepared via Precipitating a Copolymer Concentration of 1.8 wt % in DMSO into Ammonia-Containing Diethyl Ether)[a]

entry	copolymer	S_{BET} (m^2/g)
1	P($EVImBr_{1.04}$-*co*-AA)	230
2	P($CMVImBr_{1.03}$-*co*-AA)	190
3	P($BVImBr_{0.99}$-*co*-AA)	185
4	P($BzVImBr_{0.96}$-*co*-AA)	130
5	P(CMVIm$[PF_6]_{1.03}$-*co*-AA)	180
6	P(CMVIm$[Tf_2N]_{1.03}$-*co*-AA)	195

[a] PF_6: hexafluorophosphate; Tf_2N: bis(trifluoro-methanesulfonyl)-amide.

Porous polymeric materials as well as IL based materials have shown high potential in CO_2 adsorption and/or utilization approaches.[34,35] Previously, we studied the CO_2 adsorption properties of a mesoporous PIL, which has been prepared by hard-templating. Some evidence was found for CO_2−PIL interaction beyond pure surface adsorption.[27] Hence, there is strong interest to study the CO_2 sorption properties of PIL-type complexes. CO_2 sorption in PILs has been discussed heavily in the past years, and there is a general agreement on the fact that PILs seem to have a significant CO_2-philicity, which is just about to be understood.[36−38]

P($CMVImBr_{1.03}$-*co*-AA) was chosen for a more thorough investigation of its CO_2 adsorption properties. In order to understand also the effect of the interplay between the imidazolium and the carboxylate on the adsorption, some analogous systems such as nonporous P(CMVImBr) and P(CMVIm-OAc) homopolymers and a mesoporous polyelectrolyte complex prepared from P(CMVIm-Tf_2N) and PAA were also investigated (see chemical structures in Scheme S1).[26]

From previous experiments on mesoporous PILs it is known that the equilibration time can have an impact on the observed CO_2 uptake. Hence, all adsorption experiments presented in the following were made using two different measurement modes of the volumetric adsorption apparatus (see the Experimental Section). First, the measurements were conducted using the default settings of the machine. Those measurements are designated as *fast* measurements in the following. Second, the equilibration settings were set to the maximum in order to access a potentially underlying slow absorption process. Those measurements are designated as *slow* measurements in the following.

Figure 4 shows the CO_2 adsorption/desorption isotherms of P($CMVImBr_{1.03}$-*co*-AA) (Entry 2 in Table 1) obtained at 273 and 283 K. The difference between the measurement modes is quite obvious. The fast adsorption/desorption isotherms do not show any pronounced hysteresis, while a very strong hysteresis is found for the slow measurements (Figure 4A). The isosteric heats of adsorption/desorption of the fast measurements are in the range of 25−30 kJ mol^{-1}, which is a common range for physisorption of CO_2 at polar surfaces. Hence, it can be stated that the fast measurement does only represent the CO_2 adsorption at the outer surface of the mesoporous polyampholyte material.

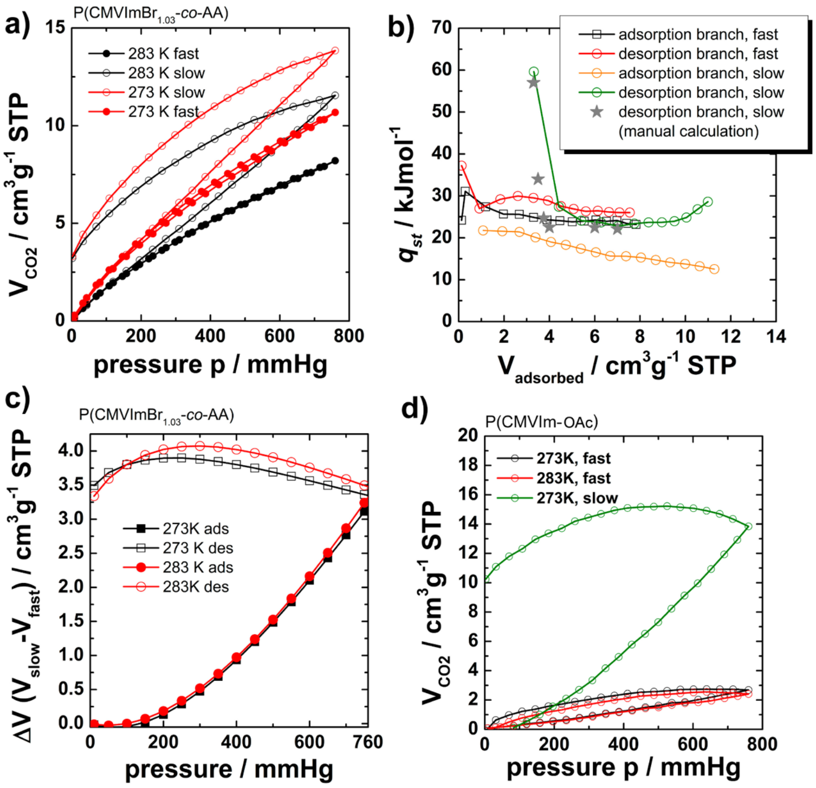

Figure 4. a) CO_2 adsorption/desorption isotherms of P($CMVImBr_{1.03}$-co-AA) (Entry 2 in Table 1) obtained at different temperatures and equilibration settings (closed symbols: fast; open symbols: slow); b) isosteric heats of CO_2 sorption; c) difference isotherm obtained by subtraction of the fast isotherm from the slow isotherms; d) CO_2 adsorption isotherms of bulk P(CMVIm-OAc) at different conditions (see the SI for isotherm plots of n_{CO2} vs pressure).

In contrast, the slow measurements give a different picture. The observed hysteresis upon desorption does not close even at very low pressures, which indicates that it is not due to simple physisorption at the surface. Furthermore, the total amount adsorbed at 760 mmHg depends on the measurement temperature, while the amount of CO_2, which could not be desorbed under the chosen equilibrium conditions, is the same for both temperatures. This finds its reflection in the isosteric heats of adsorption/desorption, which were calculated from the isotherms. The isosteric heat of slow adsorption declines from 20 kJ mol^{-1} at low coverage to 11 kJ mol^{-1} at high coverage, which is significantly (~5 to 10 kJ mol^{-1}) lower compared to the fast adsorption process. Such a low enthalpy could be explained by two overlaying contributions, namely gas binding and matrix reorganization. Although those contributions cannot be distinguished experimentally, it was shown theoretically that both are present upon dissolution of gases in rubbery polymers.[39] Van der Vegt et al. estimated the binding enthalpy of CO_2 in siloxane polymers to ~−24 kJ mol^{-1}, while the reorganization enthalpy was calculated to ~12 kJ mol^{-1}.[39] Thus, the overall CO_2 heat of adsorption ($q_{st} = -\Delta H_{ads}$) is ~12 kJ mol^{-1}, which is very close to the values calculated here, and indicates that a true carbon dioxide solubility (including polymer rearrangements) is observed here. Once the CO_2 made its way into the PIL matrix, it seems to be bound rather strongly, which is evidenced by the fact that both isotherms do not show closure of the hysteresis.

Interestingly, the heat of slow desorption was very much comparable to the fast process until the low coverage region is reached. At ~4 cm^3 g^{-1} STP the calculated heats showed a sharp increase, indicative of a strong binding. The determination of the heat of desorption was finally not possible below 3.5 cm^3 g^{-1} STP as CO_2 did not desorb within the given pressure regime and equilibration settings (CO_2 did also not desorb at 273 K down to pressures of 0.4 mbar within a time frame of >2 weeks, see the SI). Overall, the data discussed so far reveal two processes to be present: *adsorption* at the surface as a fast process and *absorption/chemisorption* within the PIL-based material as the slow process. While adsorption at the surface is quite well understood, the absorption into the polymeric matrix is of more interest in the following.

An attempt was made to separate the contributions by subtraction of the fast isotherm from the slow one (Figure 4c). To do so, the experimental isotherms were fitted using Langmuir or dual-site approaches (see the SI), and the difference isotherm ΔV was calculated by subtracting the isotherms calculated based on the fitting parameters. The corresponding isotherms look very much the same at 273 and 283 K. Both are characterized by an induction period at low pressure followed by a linear uptake of gas, which cannot be desorbed anymore. The shape of the difference isotherm is comparable to that of an adsorption/desorption isotherm of a nonporous (S_{BET} < 10 m^2 g^{-1}) P(CMVIm-OAc) polymer (Figure 4d). This polymer, which has loose acetate counterions instead of the polymeric acrylic acid carboxylate of the mesoporous polyampholyte material, does also show a large desorption hysteresis as well as a slow absorption mode (evidenced by the difference of the adsorption isotherms depending on the equilibration settings). Interestingly, the adsorption power of this polymer was much higher than that of the corresponding bulk P(CMVIm-Br) polymer. The unusual adsorption behavior of imidazolium-acetate ionic liquids with regard to CO_2 is well-known and was subject to intense investigations.[40−43] Basically, the acetate counterion can act as a base and deprotonate the imidazolium ring to form a transient N-heterocyclic carbene, which can react with CO_2 to form a carboxylate-imidazolium zwitterion (see the upper part of Scheme 1).

Scheme 1. Supposed Mechanism of CO_2 Fixation in Imidazolium-Carboxylate Based Poly(ionic liquid) Systems, Note the Necessity of Chain Rearrangements upon CO_2 Binding

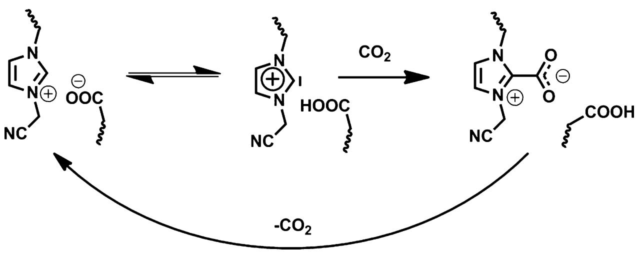

Usually, high CO_2 pressures are used and interest arose, whether the observed hysteresis could still be due to the above-described mechanism. A simple ATR-FTIR experiment was conducted to answer the question. First, the nonporous polymer P(CMVIm-OAc), which showed the stronger binding, was degassed under vacuum at 80 °C and subjected to a CO_2 atmosphere for ~20 h. The IR characteristics of the sample were measured using an ATR-FTIR setup. The spectrum was dominated by free CO_2, although there were already indications of bound CO_2. Accordingly, the sample was shortly evacuated to remove excess CO_2 and subjected again to the ATR-FTIR measurement. While being kept in the ATR setup, the sample was purged with N_2 flow using a funnel. IR spectra were recorded after 2 and 4 min of purge. All IR data are presented in Figure 5 together with the spectra of the degassed and N_2 loaded P(CMVIm-OAc).

Free CO_2 is known to show two major bands, antisymmetric stretching (ν_3) at roughly 2335 cm^{-1} and bending (ν_2) at around 669 cm^{-1}.[44] The ATR setup used here is not very convenient for the discussion of the ν_3 band and this band is hence just an indicator, whether free (noninteracting) CO_2 is present or not. In contrast, the ν_2 band is sensitive to changes of the environment, and it was shown previously that CO_2, which undergoes specific interaction with polar groups of polymers, exhibits two additional bands at lower wavenumbers as a consequence of the changed symmetry.[44] We observed the presence of ν_2 bands, characteristic of interacting CO_2 at 650 cm^{-1} next to the ν_2 band of free CO_2. A more detailed analysis is however not possible, as the parent polymer shows IR absorption in this range as well. Nevertheless, this gives evidence of CO_2 absorbed *within* the polymer matrix and does backup the gas adsorption results. The CO_2 bands are generally decreasing in intensity upon purging with N_2, which is in accordance with a physisorption model.

Analysis of the carbonyl region showed a new band at 1654 cm^{-1}, which cannot be related to free CO_2 but to CO_2 bound as carboxylate to the imidazolium ring.[40] This provides evidence for the above speculation. Usually, the reaction can easily be reversed (decarboxylation) by humidity or thermal decomposition, which is in accordance with the fact that the polymers can be regenerated by degassing at 80 °C under high vacuum to allow for full regain of adsorption capacity.

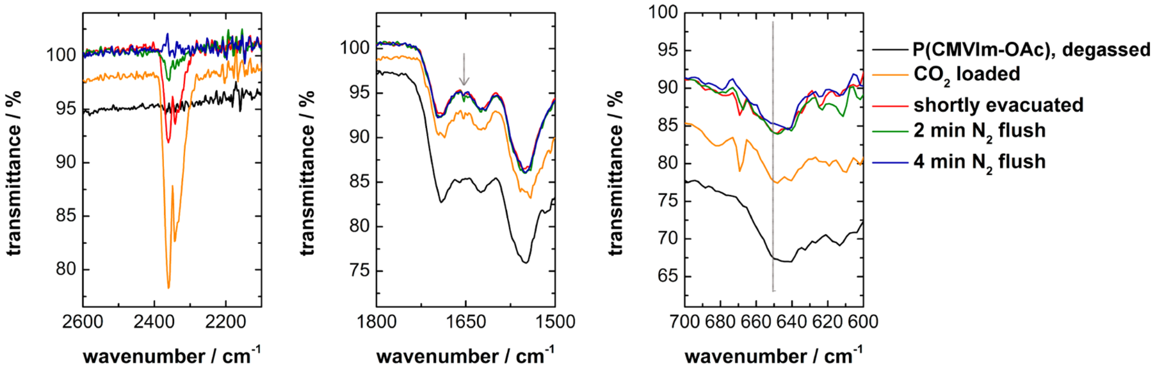

Figure 5. FTIR spectra of pure and CO_2 loaded P(CMVIm-OAc), left-hand side: characteristic region of free CO_2 (ν_3 band, ATR setup); center: carbonyl region, the arrow indicated the new band at 1654 cm^{-1} (cf. ref 40); right-hand side: ν_2 region of CO_2; the gray line indicates the ν_2 band of CO_2 absorbed in the matrix (cf. ref 44).

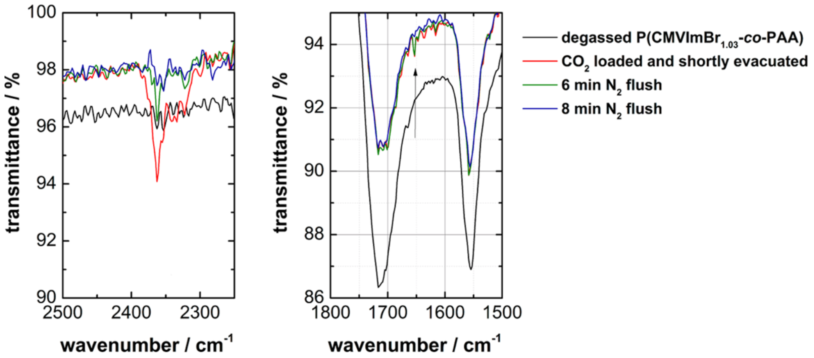

Figure 6. Left-hand side: characteristic region of free CO_2 (ν_3 band, ATR setup); right-hand side: detail of the carbonyl region showing the weak peak at 1653 cm^{-1} (cf. ref 40).

Figure 6 shows the corresponding ATR-FTIR spectra of porous P(CMVimBr$_{1.03}$-*co*-AA) loaded with CO_2 and subjected to N_2 purge together with the spectrum of the pure polymer. Again, a weak but reproducible peak can be seen at 1653 cm^{-1}. The peak is of lower intensity compared to the acetate containing PIL, which is in accordance with the higher CO_2 uptake of the acetate homopolymer.

Finally, it is worth noting that a porous poly(ionic liquid) based material that was prepared via interpolyelectrolyte complexation using cationic PIL PCMVImTf$_2$N (Tf$_2$N stands for bis(trifluoro-methanesulfonyl)amide anion) and PAA[26] showed a CO_2 adsorption/desorption behavior (including nonclosing hysteresis), which was very much the same as that of the materials described here (see the SI). This provides evidence that the underlying CO_2 binding/activation process is indeed due to the molecular characteristics of the ion pair imidazolium/carboxylate fixed in the polymer matrix and the associated intermediate NHC.

4. CONCLUSIONS

In conclusion, we presented a unique type of mesoporous polymers. The intra/intermolecular complexation of imidazolium and carboxylic acid groups, which are combined into a copolymer, leads to a fixed nanoparticulate structure upon precipitation in basic organic medium. Interstitial voids are left open as mesopores of 6−12 nm in diameter and specific surface areas up to 260 m^2 g^{-1} can be achieved. The fine chemical details of the polymer backbone (ratio imidazolium/COOH) as well as the conditions of the precipitation process are shown to control the overall porosity.

The CO_2 adsorption behavior of such permanently porous materials prepared from a single copolymer were analyzed in detail using one of them as a model compound. Next to fast CO_2 adsorption to the surface (which is the predominant mechanism in typical microporous organic polymers, such as CMPs, PIMs, etc.), additional *absorption* into the polymeric matrix was observed. This process is slow compared to the surface adsorption and comes with an energetic penalty, which is most probably due to necessary chain reorganizations. It was observed that such absorbed CO_2 could not be desorbed easily, which lead us to speculate about chemical fixation of CO_2. Indeed, the analysis of the FTIR spectra of CO_2 loaded polymers provided evidence that the trapped CO_2 can be activated to form imidazolium-carboxylate zwitterions even at low temperature and pressure. We believe the mechanism to be comparable with the previously reported formation of transient N-heterocyclic carbene species within low-molecular ionic liquids of the imidazolium-carboxylic anion type. The present system hence might provide a new way to generate heterogeneous N-heterocyclic carbenes (NHCs)[45] and can find use in a variety of applications such as catalysis. Indeed, the synthesis of heterogeneous (immobilized) NHCs is a topic of current interest and various; however, more complex ways have already been reported.[46−48] Due to the fact that the carboxylate anion is fixed to the imidazolium within the same polymer chain, we furthermore expect that leaching or ion exchange problems could be reduced. The possibility of the interaction of the carboxylate anions with CO_2 in nonimidazolium based systems should also not be discarded in future studies, as there are additional hints on such interactions.[49] They are however less explored yet and await more thorough investigation in the future. Finally, the permanent porosity does finally provide fast mass transfer, which is an additional benefit.

■ ASSOCIATED CONTENT

Ⓢ Supporting Information

Additional characterization data (NMR, elemental analysis, gas adsorption and IR data, data evaluation) are presented. This material is available free of charge via the Internet at http://pubs.acs.org.

■ AUTHOR INFORMATION

Corresponding Author

*Fax: +49-(0)331-5679502. E-mail: jens.weber@mpikg.mpg.de (J.W.), jiayin.yuan@mpikg.mpg.de (J.Y.).

Author Contributions

The manuscript was written through contributions of all authors. All authors have given approval to the final version of the manuscript.

Notes

The authors declare no competing financial interest.

■ ACKNOWLEDGMENTS

The authors thank the Max Planck Society for financial support.

■ ABBREVIATIONS

NHC: N-heterocyclic carbene; PILs: polymerized ionic liquids or poly(ionic liquid)

■ REFERENCES

(1) Yuan, J.; Antonietti, M. *Polymer* **2011**, *52*, 1469.

(2) Mecerreyes, D. *Prog. Polym. Sci.* **2011**, *36*, 1629.

(3) Lu, J.; Yan, F.; Texter, J. *Prog. Polym. Sci.* **2009**, *34*, 431.

(4) Green, M. D.; Long, T. E. *Polym. Rev.* **2009**, *49*, 291.

(5) Green, O.; Grubjesic, S.; Lee, S.; Firestone, M. A. *Polym. Rev.* **2009**, *49*, 339.

(6) Yuan, J.; Schlaad, H.; Giordano, C.; Antonietti, M. *Eur. Polym. J.* **2011**, *47*, 772.

(7) Zhao, Q.; Fellinger, T.-P.; Antonietti, M.; Yuan, J. *Macromol. Rapid Commun.* **2012**, *33*, 1149.

(8) Ohno, H. *Macromol. Symp.* **2007**, *249−250*, 551.

(9) Carlisle, T. K.; Bara, J. E.; Lafrate, A. L.; Gin, D. L.; Noble, R. D. *J. Membr. Sci.* **2010**, *359*, 37.

(10) Zhao, F.; Meng, Y.; Anderson, J. L. *J. Chromatogr., A* **2008**, *1208*, 1.

(11) Lambertus, G. R.; Crank, J. A.; McGuigan, M. E.; Kendler, S.; Armstrong, D. W.; Sacks, R. D. *J. Chromatogr., A* **2006**, *1135*, 230.

(12) Vijayakrishna, K.; Mecerreyes, D.; Gnanou, Y.; Taton, D. *Macromolecules* **2009**, *42*, 5167.

(13) Vijayakrishna, K.; Jewrajka, S. K.; Ruiz, A.; Marcilla, R.; Pomposo, J. A.; Mecerreyes, D.; Taton, D.; Gnanou, Y. *Macromolecules* **2008**, *41*, 6299.

(14) Ciferri, A.; Kudaibergenov, S. *Macromol. Rapid Commun.* **2007**, *28*, 1953.

(15) Dobrynin, A. V.; Colby, R. H.; Rubinstein, M. *J. Polym. Sci., Part B: Polym. Phys.* **2004**, *42*, 3513.

(16) Lowe, A. B.; McCormick, C. L. *Chem. Rev.* **2002**, *102*, 4177.

(17) Yamakov, V.; Milchev, A.; Limbach, H. J.; Dünweg, B.; Everaers, R. *Phys. Rev. Lett.* **2000**, *85*, 4305.

(18) Paul, G. H.; Jean-Francois, J. *J. Chem. Phys.* **1991**, *94*, 1543.

(19) Andrey, V. D.; Michael, R. *J. Phys. II* **1995**, *5*, 677.

(20) English, A. E.; Mafe, S.; Manzanares, J. A.; Yu, X.; Grosberg, A. Y.; Tanaka, T. *J. Chem. Phys.* **1996**, *104*, 8713.

(21) Schüth, F. *Chem. Mater.* **2001**, *13*, 3184.

(22) Schüth, F.; Schmidt, W. *Adv. Eng. Mater.* **2002**, *4*, 269.

(23) Yan, F.; Texter, J. *Angew. Chem., Int. Ed.* **2007**, *119*, 2492.

(24) Yan, F.; Texter, J. *Chem. Commun.* **2006**, 2696.

(25) Huang, J.; Tao, C.-a.; An, Q.; Zhang, W.; Wu, Y.; Li, X.; Shen, D.; Li, G. *Chem. Commun.* **2010**, *46*, 967.

(26) Zhao, Q.; Zhang, P.; Antonietti, M.; Yuan, J. *J. Am. Chem. Soc.* **2012**, *134*, 11852.

(27) Wilke, A.; Yuan, J.; Antonietti, M.; Weber, J. *ACS Macro Lett.* **2012**, 1028.

(28) Zhao, Q.; Soll, S.; Antonietti, M.; Yuan, J. *Polym. Chem.* **2013**, *4*, 2432−2435.

(29) Wang, Y.; Hosta-Rigau, L.; Lomas, H.; Caruso, F. *Phys. Chem. Chem. Phys.* **2011**, *13*, 4782.

(30) Wang, Y.; Yu, A.; Caruso, F. *Angew. Chem., Int. Ed.* **2005**, *44*, 2888.

(31) Yuan, J.; Giordano, C.; Antonietti, M. *Chem. Mater.* **2010**, *22*, 5003.

(32) Marcilla, R.; Alberto Blazquez, J.; Rodriguez, J.; Pomposo, J. A.; Mecerreyes, D. *J. Polym. Sci., Part A: Polym. Chem.* **2004**, *42*, 208.

(33) Dickmeis, M.; Ritter, H. *Macromol. Chem. Phys.* **2009**, *210*, 776.

(34) See, for example: (a) Chen, Q.; Luo, M.; Hammershøj, P.; Zhou, D.; Han, Y.; Laursen, B. W.; Yan, C.-G.; Han, B.-H. *J. Am. Chem. Soc.* **2012**, *134*, 6084. (b) Dawson, R.; Ratvijitvech, T.; Corker, M.; Laybourn, A.; Khimyak, Y. Z.; Cooper, A. I.; Adams, D. J. *Polym. Chem.* **2012**, *3*, 2034. (c) Kiskan, B.; Antonietti, M.; Weber, J. *Macromolecules* **2012**, *45*, 1356. (d) Wilke, A.; Weber, J. *J. Mater. Chem.* **2011**, *21*, 5226. (e) Du, N.; Park, H. B.; Robertson, G. P.; Dal-Cin, M. M.; Visser, T.; Scoles, L.; Guiver, M. D. *Nat. Mater.* **2011**, *10*, 372. (f) Luo, Y.; Li, B.; Wang, W.; Wu, K.; Tan, B. *Adv. Mater.* **2012**, *24*, 5703.

(35) (a) Bara, J. E.; Hatakeyama, E. S.; Gabriel, C. J.; Zeng, X.; Lessmann, S.; Gin, D. L.; Noble, R. D. *J. Membr. Sci.* **2008**, *316*, 186. (b) Zhu, X.; Chai, S.; Tian, C.; Fulvio, P. F.; Han, K. S.; Hagaman, E. W.; Veith, G. M.; Mahurin, S. M.; Brown, S.; Liu, H.; Dai, S. *Macromol. Rapid Commun.* **2013**, *34*, 452. (c) Zhu, X.; Hillesheim, P. C.; Mahurin, S. M.; Wang, C.; Tian, C.; Brown, S.; Luo, H.; Veith, G. M.; Han, K. S.; Hagaman, E. W.; Liu, H.; Dai, S. *ChemSusChem* **2012**, *5*, 1912.

(36) Tang, J.; Sun, W.; Tang, H.; Radosz, M.; Shen, Y. *Macromolecules* **2005**, *38*, 2037.

(37) Tang, J.; Tang, H.; Sun, W.; Radosz, M.; Shen, Y. *Polymer* **2005**, *46*, 12460.

(38) Tang, J.; Tang, H.; Sun, W.; Radosz, M.; Shen, Y. *J. Polym. Sci., Part A: Polym. Chem.* **2005**, *43*, 5477.

(39) van der Vegt, N. F. A.; Kusuma, V. A.; Freeman, B. D. *Macromolecules* **2010**, *43*, 1473.

(40) Van Ausdall, B. R.; Glass, J. L.; Wiggins, K. M.; Aarif, A. M.; Louie, J. *J. Org. Chem.* **2009**, *74*, 7935.

(41) Blath, J.; Deubler, N.; Hirth, T.; Schiestel, T. *Chem. Eng. J.* **2012**, *181−182*, 152.

(42) Cabaço, M. I.; Besnard, M.; Danten, Y.; Coutinho, J. A. P. *J. Phys. Chem. A* **2012**, *116*, 1605.

(43) Carvalho, P. J.; Álvarez, V. H.; Schröder, B.; Gil, A. M.; Marrucho, I. M.; Aznar, M.; Santos, L. M. N. B. F.; Coutinho, J. A. P. *J. Phys. Chem. B* **2009**, *113*, 6803.

(44) Kazarian, S. G.; Vincent, M. F.; Bright, F. V.; Liotta, C. L.; Eckert, C. A. *J. Am. Chem. Soc.* **1996**, *118*, 1729.

(45) Fevre, M.; Pinaud, J.; Leteneur, A.; Gnanou, Y.; Vignolle, J.; Taton, D.; Miqueu, K.; Sotiropoulos, J.-M. *J. Am. Chem. Soc.* **2012**, *134*, 6776.

(46) Pinaud, J.; Vignolle, J.; Gnanou, Y.; Taton, D. *Macromolecules* **2011**, *44*, 1900.

(47) Thiel, K.; Zehbe, R.; Roeser, J.; Strauch, P.; Enthaler, S.; Thomas, A. *Polym. Chem.* **2013**, *4*, 1848.

(48) Zeitler, K.; Mager, I. *Adv. Syn. Catal.* **2007**, *349*, 1851.

(49) (a) Kim, N.-S.; Jeong, S.-K.; Yoon, S.-H.; Park, G.-S. *Bull. Korean Chem. Soc.* **2011**, *32*, 4441. (b) Steckel, J. A. *J. Phys. Chem. A* **2012**, *116*, 11643.